Supplementary information for 'Energy versus information based estimations of dissipation using a pair of magnetic colloidal particles'

S. Tusch[2], A. Kundu[1], G. Verley[1], T. Blondel[1], V. Miralles[2], D. Démoulin[2], D. Lacoste[1], J. Baudry[2]
[1] *Laboratoire de Physico-Chimie Théorique - UMR CNRS Gulliver 7083, ESPCI, 10 rue Vauquelin, F-75231 Paris, France and*
[2] *Laboratoire LCMD, ESPCI, 10 rue Vauquelin, F-75231 Paris, France*
(Dated: April 16, 2014)

I. INTERACTION POTENTIAL BETWEEN THE BEADS

We use the 2D relative displacement vector in polar coordinates $\mathbf{r} = (r, \theta)$ as shown in (fig1). The interaction between the beads is modeled using a potential, which is the sum of three contributions: the dipolar interaction of the magnetic beads with each other U_{dip}, the interaction U_{mag} of the beads with the applied magnetic field $\mathbf{B} = B\hat{z}$, and a repulsive interaction of electrostatic origin U_{el}:

$$U(r, \theta, B) = U_{dip}(B, r, \theta) + U_{mag}(B) + U_{el}(r). \quad (1)$$

This potential has a short range repulsive part due to the electrostatics and a long-range attractive part due to the dipolar interaction as described in [**?**]. It is expressed in units of k_BT. We provide below the values of the experimental parameters entering in this potential corresponding to the $\tau = 2$s experiment described in the main text.

The electrostatic part of the potential is obtained from Debye-Hückel theory adapted to the case of two spheres using the Derjaguin approximation. In the present case, where the particle diameter d is much larger than the Debye length λ_{DB}, the expression is

$$U_{el}(r) = U_0 \ln\left(1 + e^{-(r-d)/\lambda_{DB}}\right), \quad (2)$$

where U_0 is the strength of the interaction, which depends on the particle electrostatic potential (zeta potential), the dielectric constant of the bead and the particle diameter. In the present experiment, we obtain from the fit of the probability distribution of the relative displacement between the beads: $U_0 \simeq 1800$ in units of k_BT, $d = 2.805\mu$m, and $\lambda_{DB} = 44.2$nm.

The magnetic dipolar part of the potential has the form

$$U_{dip}(B, r, \theta) = \left(\frac{B}{B_0}\right)^2 \left(\frac{d}{r}\right)^3 \left(1 - 3\cos^2\theta\right), \quad (3)$$

where B is the applied magnetic field and $B_0 = 0.09008$mT. In this model, U_{dip} describes the interaction between the two magnetic dipoles $\mathbf{m}_1$ and $\mathbf{m}_2$ carried by the beads. As mentioned in the main text, since the value of the applied field is rather large (the corresponding energy is large with respect to k_BT), we can consider that the orientation of these dipoles is frozen along the applied magnetic field. Furthermore, we assume that these dipoles are independent of the bead distance and that the two beads are identical (in particular that they have the same radius) which implies that $\mathbf{m}_1 = \mathbf{m}_2 = m\hat{z}$. In the end, the constant $(B/B_0)^2$ represents in fact $m^2/4\pi\mu_0$, given the linear relation between the magnetic dipoles and the applied magnetic field.

The direct interaction of the magnetic dipoles $\mathbf{m}_1$ and $\mathbf{m}_2$ carried by both beads with the magnetic field is

$$U_{mag}(B) = -\mathbf{m}_1 \cdot \mathbf{B} - \mathbf{m}_1 \cdot \mathbf{B}, \quad (4)$$

Given our assumption that $\mathbf{m}_1 = \mathbf{m}_2$ independent of r, this term represents a contribution which is quadratic in the field but constant in terms of the r dependence.

II. HYDRODYNAMIC MODEL OF THE FRICTION BETWEEN THE BEADS

Dissipation in this system is mainly of hydrodynamic origin. In view of the proximity of the two beads with respect to each other and to the wall, one can rely on the lubrication approximation to describe the hydrodynamic friction coefficients. These coefficients are the sum of the friction due to the sphere-sphere interaction Γ_i^s and the friction between the sphere and the bottom wall Γ_i^w, because the corresponding forces are parallel to each other. More explicitly $\Gamma_i(r) = \Gamma_i^s + \Gamma_i^w$ for $i \equiv \{r, \theta\}$. We thank H. Stone for insightful discussions concerning the proper modeling of these friction coefficients.

Let us first discuss the friction between the spheres and the wall, and to obtain that we first need to know the interaction of a single sphere with a wall. This hydrodynamic interaction can be calculated within the lubrication approximation. We are mainly interested in the case of the translation of the sphere in a tangent plane parallel to the wall (assuming no rotation of the bead). In this case, the friction is increased by a factor $16\pi \ln(a/b)/15$, where a is the bead radius and b the gap between the sphere and the wall, with respect to the Stokes-Einstein friction of the same sphere in a bulk fluid [**?**]. It follows from this that the friction coefficient between the

A. Kundu is presently employed at Laboratoire de Physique Théorique et Modèdes Statistiques - UMR CNRS 8626, Université Paris-Sud, Bât. 100, 91405 Orsay Cedex, France. G. Verley is employed at Physics and Material Sciences Research Unit, University of Luxembourg, L-1511 Luxembourg, G.D. Luxembourg.

two beads and the wall along the $\boldsymbol{e}_r$ and $\boldsymbol{e}_\theta$ directions take the following form

$$\Gamma_r^w(r) = \frac{8}{15}\gamma \ln\frac{a}{b}, \qquad (5)$$
$$\Gamma_\theta^w(r) = \frac{8}{15}\gamma r^2 \ln\frac{a}{b},$$

where γ represents the bare friction coefficient of a single bead far from the wall.

In order to model the hydrodynamic interaction between the beads, we have built our model on the work of Jeffrey and Onishi [**?**]. The first step is to reduce the motion of the two beads to the motion of one fictive particle in the frame of the center of mass. We denote by $\dot{\boldsymbol{r}}^\sigma$ the velocity vector of the magnetic bead σ and $\dot{r}_i^\sigma$ its coordinate i. The force applied on the bead is $\boldsymbol{F}^\sigma = -\nabla^\sigma V(\boldsymbol{r}^\sigma - \boldsymbol{r}^\omega) = \nabla^\omega V(\boldsymbol{r}^\sigma - \boldsymbol{r}^\omega) = -\boldsymbol{F}^\omega$ and its coordinates are F_i^σ. The symbol ∇^ω is for the gradient calculated with the coordinates of the bead ω. In the following we neglect the rotation of the beads and the hydrodynamics torque. The force and the velocity are given by

$$\dot{r}_i^\sigma = M_{ij}^{\sigma\omega} F_j^\omega, \qquad (6)$$

thanks to the linearity of the Stokes equation at low Reynolds number [**?**]. By convention, all repeated indices are summed over. The spheres being symmetric, the mobility tensor M is symmetric in the exchange of the two beads, i.e. $M_{ij}^{\sigma\omega} = M_{ij}^{\omega\sigma}$. The relative velocity of the two beads is given by the vector $\dot{\boldsymbol{r}} = \dot{\boldsymbol{r}}^1 - \dot{\boldsymbol{r}}^2$ and the coordinates of that vector verify

$$\begin{aligned}\dot{r}_i &= M_{ij}^{11}F_j^1 + M_{ij}^{12}F_j^2 - M_{ij}^{21}F_j^1 - M_{ij}^{22}F_j^2 \\ &= 2\left(M_{ij}^{11} - M_{ij}^{12}\right)F_j^1. \end{aligned} \qquad (7)$$

Using the unit vector $\boldsymbol{e}_r = \mathbf{r}/r$ of coordinates $e_1 = 1$ and $e_2 = 0$ in the polar basis $(\boldsymbol{e}_r, \boldsymbol{e}_\theta)$, the mobility tensor takes the following form

$$M_{ij}^{\sigma\omega} = x^{\sigma\omega}e_i e_j + y^{\sigma\omega}(\delta_{ij} - e_i e_j) \qquad (8)$$

where the coefficients $x^{\sigma\omega}$ and $y^{\sigma\omega}$ are dependant of the distance r between the two beads. The coordinates of the relative velocity become then

$$\dot{r}_i = 2(x^{11} - x^{12})e_i e_j F_j^1 + 2(y^{11} - y^{12})(\delta_{ij} - e_i e_j)F_j^1, \qquad (9)$$

or more explicitly because $\dot{r}_1 = \dot{r}$ and $\dot{r}_2 = r\dot{\theta}$ in polar coordinates (we have for the relative velocity in the polar basis $\dot{\mathbf{r}} = \dot{r}\boldsymbol{e}_r + r\dot{\theta}\boldsymbol{e}_\theta$).

$$\dot{r} = 2(x^{11} - x^{12})F_1^1 = -2(x^{11} - x^{12})\partial_r V(r,\theta), \qquad (10)$$
$$r\dot{\theta} = 2(y^{11} - y^{12})F_2^1 = -\frac{2(y^{11} - y^{12})}{r}\partial_\theta V(r,\theta). \qquad (11)$$

We have used the coefficients $x^{\sigma\omega}$ and $y^{\sigma\omega}$ introduced by D.J. Jeffrey and Y. Onishi [**?**] in the nearly touching sphere limit [**?**]. In this limit, we have

$$x^{11} - x^{12} = \frac{4}{\gamma}\left(\frac{r}{d} - 1\right), \qquad (12)$$
$$y^{11} - y^{12} = \frac{0.402(\ln\xi^{-1})^2 + 2.96\ln\xi^{-1} + 5.09}{\gamma\left((\ln\xi^{-1})^2 + 6.04\ln\xi^{-1} + 6.33\right)}, \qquad (13)$$

where $\xi = 2(r-d)/d = (r-2a)/a$ and $\gamma = 6\pi\eta d/2 = 6\pi\eta a$ the friction coefficient of one particle alone in the fluid of viscosity η. In order to obtain a compact notation, we introduce the notation $k(r) = \gamma(y^{11} - y^{12})$, with the $y^{11} - y^{12}$ given in the equation above. It follows that the friction coefficients for the sphere-sphere interaction take the form

$$\Gamma_r^s(r) = \frac{\gamma a}{4r - 8a}, \qquad (14)$$
$$\Gamma_\theta^s(r) = \frac{\gamma r^2}{2k(r)}.$$

When these friction coefficients are combined with the friction coefficients for the sphere-wall interaction given in Eq. 5, the full friction tensor and the Langevin equations given in the main text are obtained.

III. DISTRIBUTIONS OF HEAT AND INTERNAL ENERGY

We show in figures 1 and 2 the probability distributions of heat and internal energy constructed from the experimental datas used also for figure 3 of the main text. These histograms represent experimental data points which are compared with simulations of the Langevin equations.

With the definitions of work and heat of Eq. 4 of the main text, one can write the first law in the form of $\Delta U = W + Q$, where ΔU denotes the difference of internal energy between the initial and final point of the cycle namely, $U(\mathbf{r}(\tau+\tau_{eq}), B(\tau+\tau_{eq})) - U(\mathbf{r}(0), B(0))$. Now, by definition of a cyclic protocol, the initial and final value of the control parameter are the same. Since $\mathbf{r}(0)$ and $\mathbf{r}(\tau+\tau_{eq})$ are distributed according to the same canonical distribution (if the equilibration is done properly), then it follows that $\langle\Delta U\rangle = \langle W\rangle + \langle Q\rangle = 0$. This is indeed well verified by the experimental average work and heat, since we have obtained $\langle W\rangle = 3.3 \pm 0.2 k_B T$ and $\langle Q\rangle = -3.4 \pm 0.2 k_B T$. Naturally, higher moments of the distribution of the random variable ΔU may not vanish. In fact, as mentioned in the main text, a strategy to test that the system is well equilibrated with a sufficient duration of the pauses consists precisely in studying this distribution of internal energy and in comparing it with the heat fluctuations measured at equilibrium. Indeed, for a constant value of the magnetic field, we measure the equilibrium distribution of heat, denoted $P_{eq}(Q)$. Since there is no work in this case, this distribution $P_{eq}(Q)$ should match $P(\Delta U)$ in the non-equilibrium experiment provided the initial and end point in the cycle in the

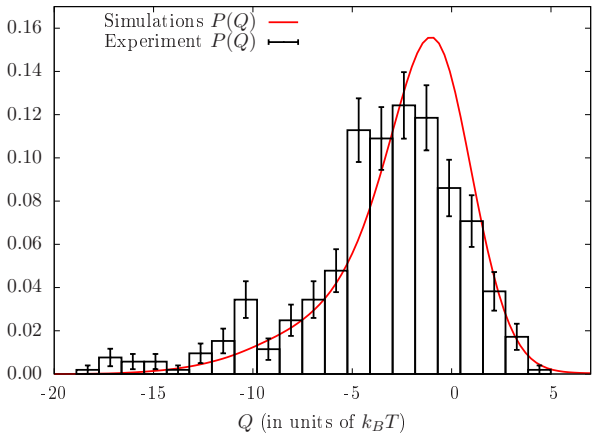

FIG. 1. Probability distribution of the heat $P(Q)$, constructed from an experiment using 460 cycles (histogram) and from a simulation of Eq. 2 of the main text (solid line), in the same conditions as the probability distribution of work shown in Fig 3 of the main text. The average heat in this experiment is $-3.4 \pm 0.2 k_B T$.

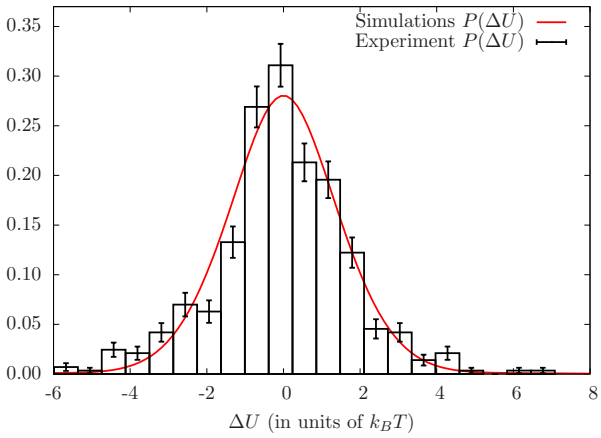

FIG. 2. Probability distribution of the internal energy $P(\Delta U)$, constructed from an experiment using 460 cycles (histogram) and from a simulation of Eq. 2 of the main text (solid line), in the same conditions as in Fig 1 of the main text. The average internal energy in this experiment is close to zero.

non-equilibrium experiment are well equilibrated and if the control parameter at these points has the same value as the one used in the equilibrium experiment. Therefore, as mentioned in the text, a comparison between these two distributions offers a simple way to test equilibration in this system. As shown in fig 3, this test is well satisfied in the conditions of our experiment.

We have also studied the approach to the quasi-static limit using simulations. Using simulations, we have evaluated $\langle W \rangle$ for different durations τ of the protocol. As expected $\langle W \rangle \to 0$ in the quasi-static limit $\tau \to \infty$ and in the limit $\tau \to 0$ by definition. As a result, we find that $\langle W \rangle$ has a maximum at some τ which depends on equilibration time τ_{eq} and on the relaxation time τ_{rel} characteristic of the fluctuations around the minimum of the potential. Since the potential is very anharmonic, $\tau_{eq} \gg \tau_{rel}$. We have also observed that the maximum of $\langle W \rangle$ occurs at a time which is too short to be accessible with our experiment.

A few words on how the experimental histograms have been constructed: The histograms have been obtained by counting the number of events n_i with a work, heat or energy change in the range of the ith bar of the histogram, i.e. $p_i = n_i/N$ with N the total number of events. The error bars are estimated using the variance of the binomial law for the random variable n_i leading to the following approximation for p_i, namely $n_i/N \pm (p_i(1-p_i)/N)^{1/2}$.

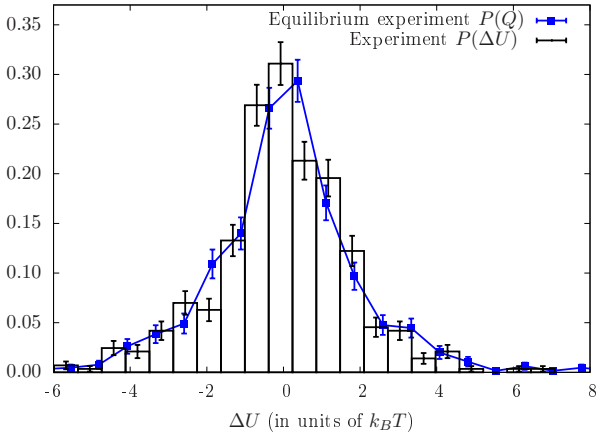

FIG. 3. Probability distribution of the internal energy change $P(\Delta U)$, constructed from non equilibrium experiments using 460 cycles (histogram) and probability distribution of heat exchange from equilibrium experiments (continuous line with data points).

IV. INFORMATION BASED ESTIMATION OF THE AVERAGE DISSIPATION

The first method discussed in the main text, to estimate the dissipation from the information content of the trajectories, relies on an estimate of the KL divergence of two probability distributions $p_F(t)$ and $p_R(\tau - t)$, evaluated at two points which are time-reversal symmetric in the protocol of applied magnetic field. We recall the inequality which is used:

$$\beta \langle W_{diss}(\tau) \rangle \geq D(p_F(t) || p_R(\tau - t)). \qquad (15)$$

In order to test this idea, we have evaluated the left and the right hand side of this equation at different time t, which corresponds to the time of a specific point within the protocol of duration τ as defined in figure 1. Due to the symmetry of the protocol, the average dissipated work $\langle W_{diss}(\tau)\rangle$ is equal to the average work $\langle W(\tau)\rangle$ measured in the first part of the paper. For completeness, we include here two snapshots of the probabilities used to determine the KL estimate, at two specific times, namely at $t = 1.5$s and $t = 2$s. On one hand, at the time $t = 1.5$s, the KL divergence is close to its maximum as shown in Fig. 4 of the main text, and we can see in figure 4 that indeed the two distributions differ significantly from each other at this time. On the other hand, at the time $t = 2$s, the two distributions are closer to each other as seen in figure 5 and as a result the KL estimate is lower. It is interesting to note that in Fig. 4, the highest value of the KL divergence occurs in the second half of the protocol, only after the protocol has changed sign. This shows that the irreversibility of the evolution of the system is easier to determine from the information of the trajectories only after the system has reacted to a variation of the protocol in time.

The second method to estimate dissipation from the information of the trajectories discussed in the main text relies instead on an estimate of the KL divergence between an equilibrium $p_{eq}(t)$ and a non-equilibrium probability distribution $p_{neq}(t)$. In such a formulation, both distributions need to be evaluated at the current value of the control parameter at time t which is the final time for the evaluation of the dissipated work $W_{diss}(t)$:

$$\beta\langle W_{diss}(t)\rangle \geq D(p_{neq}(t)||p_{eq}(t)). \tag{16}$$

In order to test this relation, we have again varied the time t as before. In such a case, since the protocol is no longer symmetric, i.e. it does not take the same value at the initial and final time used in the evaluation of $\langle W_{diss}(t)\rangle$, one needs to take into account the contribution from the free energy. Thus, we evaluate $\langle W_{diss}(t)\rangle$ from $\langle W(t)\rangle - \Delta F(t)$, where $\Delta F(t) = F(B(t)) - F(B(0))$ is the equilibrium free energy difference evaluated with a protocol taken at time t and at the initial time 0. In order to evaluate this free energy, we have calculated it numerically from the partition function as the following 2D integral $F(B) = -k_B T \log Z(B)$, where

$$Z(B) = \int d\mathbf{r} \exp\left(-\beta U(r,\theta,B)\right), \tag{17}$$

where the integrand contains the 2D interaction potential introduced in the first section of these notes. At low field, the potential is not sufficiently confining and the integral over the distance between the beads r needs to be regularized. In order to do this, we have introduced a cutoff which corresponds to the maximum distance observed in the experiment between the beads, namely a few microns. To summarize, the evaluation of $\langle W_{diss}(t)\rangle$ requires the experimentally determined values of the work on the 460 cycles used before, together with the above free energy difference evaluated with the corresponding value of the protocol of magnetic field at the time t. As expected from Eq. 16, the curve corresponding to $\langle W_{diss}(t)\rangle$ lies above the one corresponding to the KL bound at all times except in a small region at very early time. In this region, both $\langle W_{diss}(t)\rangle$ and its KL estimate are small and their precise evaluation is more difficult than at later times. We attribute the discrepancy seen at very early time to the fact that the equilibration at the initial time may not be perfect and the experimental probability distribution may differ slightly from $p_{eq}(\tau)$ which is evaluated using the theoretical model for the interaction potential.

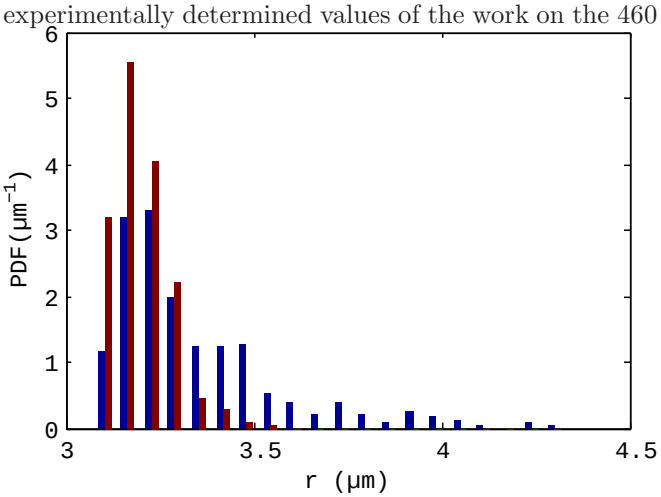

FIG. 4. Histogram of the probability distribution $p_F(t)$ (blue bars) and $p_R(\tau - t)$ (red bars) evaluated at the time $t = 1.5$.

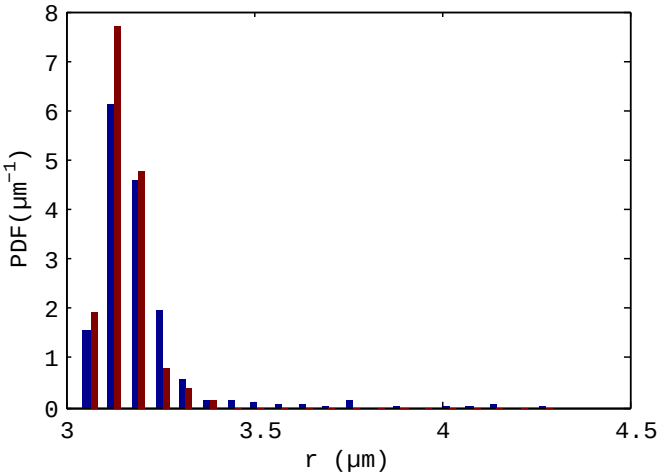

FIG. 5. Histogram of the probability distribution $p_F(t)$ (blue bars) and $p_R(\tau - t)$ (red bars) evaluated at the time $t = 2$s.